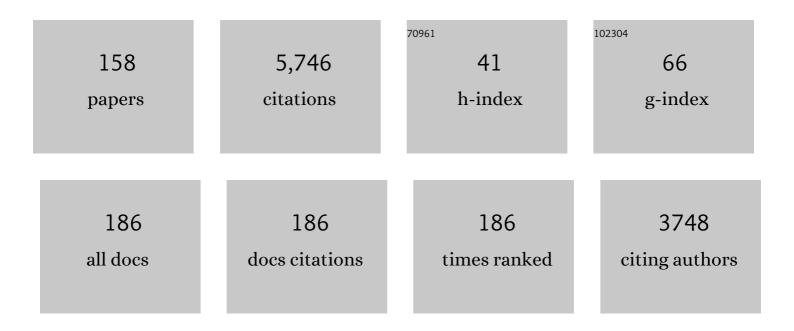
Reinhard Schweitzer-Stenner

List of Publications by Year in descending order

Source: https://exaly.com/author-pdf/294697/publications.pdf Version: 2024-02-01



#	Article	IF	CITATIONS
1	Tripeptides Adopt Stable Structures in Water. A Combined Polarized Visible Raman, FTIR, and VCD Spectroscopy Study. Journal of the American Chemical Society, 2002, 124, 14330-14341.	6.6	199
2	Dihedral Ï^ Angle Dependence of the Amide III Vibration:Â A Uniquely Sensitive UV Resonance Raman Secondary Structural Probe. Journal of the American Chemical Society, 2001, 123, 11775-11781.	6.6	185
3	Vibrational Assignments of trans-N-Methylacetamide and Some of Its Deuterated Isotopomers from Band Decomposition of IR, Visible, and Resonance Raman Spectra. The Journal of Physical Chemistry, 1995, 99, 3074-3083.	2.9	151
4	Advances in vibrational spectroscopy as a sensitive probe of peptide and protein structure. Vibrational Spectroscopy, 2006, 42, 98-117.	1.2	142
5	Stable Conformations of Tripeptides in Aqueous Solution Studied by UV Circular Dichroism Spectroscopy. Journal of the American Chemical Society, 2003, 125, 8178-8185.	6.6	140
6	Dihedral Angles of Trialanine in D2O Determined by Combining FTIR and Polarized Visible Raman Spectroscopy. Journal of the American Chemical Society, 2001, 123, 9628-9633.	6.6	130
7	Intrinsic Propensities of Amino Acid Residues in GxG Peptides Inferred from Amide l′ Band Profiles and NMR Scalar Coupling Constants. Journal of the American Chemical Society, 2010, 132, 540-551.	6.6	124
8	The Conformation of Tetraalanine in Water Determined by Polarized Raman, FT-IR, and VCD Spectroscopy. Journal of the American Chemical Society, 2004, 126, 2768-2776.	6.6	123
9	Conformational Properties of Nickel(II) Octaethylporphyrin in Solution. 1. Resonance Excitation Profiles and Temperature Dependence of Structure-Sensitive Raman Lines. The Journal of Physical Chemistry, 1996, 100, 14184-14191.	2.9	118
10	N-Methylacetamide and Its Hydrogen-Bonded Water Molecules Are Vibrationally Coupled. Journal of the American Chemical Society, 1994, 116, 11141-11142.	6.6	112
11	Preferred peptide backbone conformations in the unfolded state revealed by the structure analysis of alanine-based (AXA) tripeptides in aqueous solution. Proceedings of the National Academy of Sciences of the United States of America, 2004, 101, 10054-10059.	3.3	110
12	Vibrational Circular Dichroism as a Probe of Fibrillogenesis: The Origin of the Anomalous Intensity Enhancement of Amyloid-like Fibrils. Journal of the American Chemical Society, 2011, 133, 1066-1076.	6.6	102
13	Dihedral Angles of Tripeptides in Solution Directly Determined by Polarized Raman and FTIR Spectroscopy. Biophysical Journal, 2002, 83, 523-532.	0.2	98
14	The Structure of Alanine Based Tripeptides in Water and Dimethyl Sulfoxide Probed by Vibrational Spectroscopy. Journal of Physical Chemistry B, 2003, 107, 358-365.	1.2	93
15	Aβ1-28Fragment of the Amyloid Peptide Predominantly Adopts a Polyproline II Conformation in an Acidic Solutionâ€. Biochemistry, 2004, 43, 6893-6898.	1.2	88
16	Secondary Structure Analysis of Polypeptides Based on an Excitonic Coupling Model to Describe the Band Profile of Amide lâ€~ of IR, Raman, and Vibrational Circular Dichroism Spectra. Journal of Physical Chemistry B, 2004, 108, 16965-16975.	1.2	87
17	Inactivation of Horseradish Peroxidase by Phenoxyl Radical Attack. Journal of the American Chemical Society, 2005, 127, 1431-1437.	6.6	87
18	UV Raman Determination of the .pipi.* Excited State Geometry of N-Methylacetamide: Vibrational Enhancement Pattern. Journal of the American Chemical Society, 1995, 117, 2884-2895.	6.6	86

#	Article	IF	CITATIONS
19	The Amide I Mode of Peptides in Aqueous Solution Involves Vibrational Coupling between the Peptide Group and Water Molecules of the Hydration Shell. Journal of the American Chemical Society, 1997, 119, 1720-1726.	6.6	78
20	Distribution of Conformations Sampled by the Central Amino Acid Residue in Tripeptides Inferred From Amide I Band Profiles and NMR Scalar Coupling Constants. Journal of Physical Chemistry B, 2009, 113, 2922-2932.	1.2	78
21	Structure Analysis of Dipeptides in Water by Exploring and Utilizing the Structural Sensitivity of Amide III by Polarized Visible Raman, FTIRâ~Spectroscopy and DFT Based Normal Coordinate Analysis. Journal of Physical Chemistry B, 2002, 106, 4294-4304.	1.2	71
22	Visible and UV-resonance Raman spectroscopy of model peptides. Journal of Raman Spectroscopy, 2001, 32, 711-732.	1.2	70
23	The alanine-rich XAO peptide adopts a heterogeneous population, including turn-like and polyproline II conformations. Proceedings of the National Academy of Sciences of the United States of America, 2007, 104, 6649-6654.	3.3	65
24	pH-Independence of Trialanine and the Effects of Termini Blocking in Short Peptides: A Combined Vibrational, NMR, UVCD, and Molecular Dynamics Study. Journal of Physical Chemistry B, 2013, 117, 3689-3706.	1.2	64
25	Planar and Nonplanar Conformations of (meso-Tetraphenylporphinato)nickel(II) in Solution As Inferred from Solution and Solid-State Raman Spectroscopy. Journal of Physical Chemistry A, 1997, 101, 5789-5798.	1.1	63
26	Intermolecular Coupling in Liquid and Crystalline States of trans-N-Methylacetamide Investigated by Polarized Raman and FT-IR Spectroscopies. Journal of Physical Chemistry A, 1998, 102, 118-127.	1.1	59
27	Conformational propensities and residual structures in unfolded peptides and proteins. Molecular BioSystems, 2012, 8, 122-133.	2.9	59
28	Ultraâ€Long Crystalline Red Phosphorus Nanowires from Amorphous Red Phosphorus Thin Films. Angewandte Chemie - International Edition, 2016, 55, 11829-11833.	7.2	56
29	Conformational Manifold of α-Aminoisobutyric Acid (Aib) Containing Alanine-Based Tripeptides in Aqueous Solution Explored by Vibrational Spectroscopy, Electronic Circular Dichroism Spectroscopy, and Molecular Dynamics Simulations. Journal of the American Chemical Society, 2007, 129, 13095-13109.	6.6	55
30	Local Order in the Unfolded State: Conformational Biases and Nearest Neighbor Interactions. Biomolecules, 2014, 4, 725-773.	1.8	54
31	Allosteric linkage-induced distortions of the prosthetic group in haem proteins as derived by the theoretical interpretation of the depolarization ratio in resonance Raman scattering. Quarterly Reviews of Biophysics, 1989, 22, 381-479.	2.4	52
32	Conformations of Alanine-Based Peptides in Water Probed by FTIR, Raman, Vibrational Circular Dichroism, Electronic Circular Dichroism, and NMR Spectroscopyâ€. Biochemistry, 2007, 46, 1587-1596.	1.2	52
33	Different Conformers and Protonation States of Dipeptides Probed by Polarized Raman, UVâ ``Resonance Raman, and FTIR Spectroscopy. Journal of Physical Chemistry B, 1999, 103, 372-384.	1.2	49
34	Amino Acids with Hydrogenâ€Bonding Side Chains have an Intrinsic Tendency to Sample Various Turn Conformations in Aqueous Solution. Chemistry - A European Journal, 2011, 17, 6789-6797.	1.7	49
35	Optical Band Splitting and Electronic Perturbations of the Heme Chromophore in Cytochrome c at Room Temperature Probed by Visible Electronic Circular Dichroism Spectroscopy. Biophysical Journal, 2007, 92, 989-998.	0.2	47
36	Structure of Poly(Ethylene Glycol)-Modified Horseradish Peroxidase in Organic Solvents: Infrared Amide I Spectral Changes upon Protein Dehydration Are Largely Caused by Protein Structural Changes and Not by Water Removal Per Se. Biophysical Journal, 2002, 83, 3637-3651.	0.2	46

#	Article	IF	CITATIONS
37	Simulated IR, Isotropic and Anisotropic Raman, and Vibrational Circular Dichroism Amide I Band Profiles of Stacked I²-Sheets. Journal of Physical Chemistry B, 2012, 116, 4141-4153.	1.2	45
38	The Endogenous Calcium Ions of Horseradish Peroxidase C Are Required to Maintain the Functional Nonplanarity of the Heme. Biophysical Journal, 2003, 84, 2542-2552.	0.2	44
39	Aggregation of the Amphipathic Peptides (AAKA)ninto Antiparallel β-Sheets. Journal of the American Chemical Society, 2006, 128, 13324-13325.	6.6	44
40	Self-Aggregation of a Polyalanine Octamer Promoted by Its C-Terminal Tyrosine and Probed by a Strongly Enhanced Vibrational Circular Dichroism Signal. Journal of the American Chemical Society, 2009, 131, 18218-18219.	6.6	43
41	Coexistence of Native-like and Non-Native Partially Unfolded Ferricytochrome <i>c</i> on the Surface of Cardiolipin-Containing Liposomes. Journal of Physical Chemistry B, 2015, 119, 1334-1349.	1.2	43
42	Amyloid Precursor Protein Translation Is Regulated by a 3'UTR Guanine Quadruplex. PLoS ONE, 2015, 10, e0143160.	1.1	42
43	The Conformational Manifold of Ferricytochrome <i>c</i> Explored by Visible and Far-UV Electronic Circular Dichroism Spectroscopy. Biochemistry, 2008, 47, 9667-9677.	1.2	41
44	Assessing backbone solvation effects in the conformational propensities of amino acid residues in unfolded peptides. Physical Chemistry Chemical Physics, 2015, 17, 24917-24924.	1.3	41
45	The structure of tri-proline in water probed by polarized Raman, Fourier transform infrared, vibrational circular dichroism, and electric ultraviolet circular dichroism spectroscopy. Biopolymers, 2003, 71, 558-568.	1.2	40
46	Raman dispersion spectroscopy on the highly saddled nickel(II)-octaethyltetraphenylporphyrin reveals the symmetry of nonplanar distortions and the vibronic coupling strength of normal modes. Journal of Chemical Physics, 1997, 107, 1794-1815.	1.2	39
47	Protein Dynamics in an Intermediate State of Myoglobin: Optical Absorption, Resonance Raman Spectroscopy, and X-Ray Structure Analysis. Biophysical Journal, 2000, 78, 2081-2092.	0.2	39
48	Nonplanar Heme Deformations and Excited State Displacements in Nickel Porphyrins Detected by Raman Spectroscopy at Soret Excitation. Journal of Physical Chemistry A, 2005, 109, 10493-10502.	1.1	39
49	Side Chain Dependence of Intensity and Wavenumber Position of Amide lâ€~ in IR and Visible Raman Spectra of XA and AX Dipeptides. Journal of Physical Chemistry B, 2005, 109, 8195-8205.	1.2	39
50	Anharmonic Protein Motions and Heme Deformations in Myoglobin Cyanide Probed by Absorption and Resonance Raman Spectroscopy. Journal of Physical Chemistry B, 2000, 104, 4754-4764.	1.2	38
51	Discrepancies between Conformational Distributions of a Polyalanine Peptide in Solution Obtained from Molecular Dynamics Force Fields and Amide l′ Band Profiles. Journal of Physical Chemistry B, 2010, 114, 17201-17208.	1.2	38
52	Internal Electric Field in Cytochrome C Explored by Visible Electronic Circular Dichroism Spectroscopy Journal of Physical Chemistry B, 2008, 112, 10358-10366.	1.2	36
53	Role of Enthalpy–Entropy Compensation Interactions in Determining the Conformational Propensities of Amino Acid Residues in Unfolded Peptides Journal of Physical Chemistry B, 2014, 118, 1309-1318.	1.2	36
54	Coexistence of Native-Like and Non-Native Cytochrome <i>c</i> on Anionic Liposomes with Different Cardiolipin Content. Journal of Physical Chemistry B, 2015, 119, 12846-12859.	1.2	36

#	Article	IF	CITATIONS
55	The pH Dependence of the 695 nm Charge Transfer Band Reveals the Population of an Intermediate State of the Alkaline Transition of Ferricytochrome <i>c</i> at Low Ion Concentrations. Biochemistry, 2009, 48, 2990-2996.	1.2	35
56	Disorder and order in unfolded and disordered peptides and proteins: A view derived from tripeptide conformational analysis. II. Tripeptides with short side chains populating asx and βâ€ŧype like turn conformations. Proteins: Structure, Function and Bioinformatics, 2013, 81, 968-983.	1.5	35
57	Uncoupled Adjacent Amide Vibrations in Small Peptides. Journal of the American Chemical Society, 2000, 122, 9028-9029.	6.6	34
58	Relating the multi-functionality of cytochrome c to membrane binding and structural conversion. Biophysical Reviews, 2018, 10, 1151-1185.	1.5	34
59	Disorder and order in unfolded and disordered peptides and proteins: A view derived from tripeptide conformational analysis. I. Tripeptides with long and predominantly hydrophobic side chains. Proteins: Structure, Function and Bioinformatics, 2013, 81, 955-967.	1.5	33
60	Water-Centered Interpretation of Intrinsic pPII Propensities of Amino Acid Residues: <i>In Vitro</i> -Driven Molecular Dynamics Study. Journal of Physical Chemistry B, 2015, 119, 13237-13251.	1.2	33
61	ls a cross-β-sheet structure of low molecular weight peptides necessary for the formation of fibrils and peptide hydrogels?. Physical Chemistry Chemical Physics, 2018, 20, 18158-18168.	1.3	33
62	Cardiolipin containing liposomes are fully ionized at physiological pH. An FT-IR study of phosphate group ionization. Vibrational Spectroscopy, 2014, 75, 86-92.	1.2	32
63	Perturbation of water structure by water-polymer interactions probed by FTIR and polarized Raman spectroscopy. Journal of Molecular Liquids, 2019, 275, 463-473.	2.3	31
64	Structural Disorder of Native Horseradish Peroxidase C Probed by Resonance Raman and Low-Temperature Optical Absorption Spectroscopy. Journal of Physical Chemistry B, 2003, 107, 2822-2830.	1.2	29
65	Simulation of amide l′ band profiles of trans polyproline based on an excitonic coupling model. Chemical Physics Letters, 2005, 408, 123-127.	1.2	29
66	Salmon Calcitonin and Amyloid β: Two Peptides with Amyloidogenic Capacity Adopt Different Conformational Manifolds in Their Unfolded Statesâ€. Biochemistry, 2006, 45, 2810-2819.	1.2	29
67	Conformational Changes of Trialanine Induced by Direct Interactions between Alanine Residues and Alcohols in Binary Mixtures of Water with Glycerol and Ethanol. Journal of the American Chemical Society, 2011, 133, 12728-12739.	6.6	29
68	A New Method for Evaluating the Conformations and Normal Modes of Macromolecule Vibrations with a Reduced Force Field. 2. Application to Nonplanar Distorted Metal Porphyrins. Journal of Physical Chemistry B, 1999, 103, 10022-10031.	1.2	28
69	Conformational Analysis of XA and AX Dipeptides in Water by Electronic Circular Dichroism and1H NMR Spectroscopy. Journal of Physical Chemistry B, 2006, 110, 6979-6986.	1.2	28
70	Demixing of water and ethanol causes conformational redistribution and gelation of the cationic GAG tripeptide. Chemical Communications, 2015, 51, 16498-16501.	2.2	28
71	The importance of vibronic perturbations in ferrocytochrome c spectra: A reevaluation of spectral properties based on low-temperature optical absorption, resonance Raman, and molecular-dynamics simulations. Journal of Chemical Physics, 2005, 123, 054508.	1.2	27
72	Cutting Edge: Death of a Dogma or Enforcing the Artificial: Monomeric IgE Binding May Initiate Mast Cell Response by Inducing Its Receptor Aggregation. Journal of Immunology, 2005, 174, 4461-4464.	0.4	27

#	Article	IF	CITATIONS
73	Structural Changes of Horse Heart Ferricytochrome <i>c</i> Induced by Changes of Ionic Strength and Anion Binding. Biochemistry, 2008, 47, 5250-5257.	1.2	27
74	Randomizing the Unfolded State of Peptides (and Proteins) by Nearest Neighbor Interactions between Unlike Residues. Chemistry - A European Journal, 2015, 21, 5173-5192.	1.7	27
75	The interplay of aggregation, fibrillization and gelation of an unexpected low molecular weight gelator: glycylalanylglycine in ethanol/water. Soft Matter, 2016, 12, 6096-6110.	1.2	27
76	Multimode analysis of depolarization ratio dispersion and excitation profiles of seven Raman fundamentals from the haeme group in ferrocytochrome c. Journal of Raman Spectroscopy, 1991, 22, 65-78.	1.2	25
77	Polarized Raman dispersion spectroscopy probes planar and non-planar distortions of Ni(II) porphyrins with different peripheral substituents. Journal of Raman Spectroscopy, 1998, 29, 945-953.	1.2	25
78	Polarized resonance Raman dispersion spectroscopy on metalporphyrins. Journal of Porphyrins and Phthalocyanines, 2001, 05, 198-224.	0.4	24
79	Structure and dynamics of biomolecules probed by Raman spectroscopy. Journal of Raman Spectroscopy, 2005, 36, 276-278.	1.2	24
80	Conformational Substates of Horse Heart Cytochrome <i>c</i> Exhibit Different Thermal Unfolding of the Heme Cavity. Journal of Physical Chemistry B, 2007, 111, 9603-9607.	1.2	23
81	Kinetics of the selfâ€aggregation and film formation of polyâ€≺scp>Lâ€proline at high temperatures explored by circular dichroism spectroscopy. Biopolymers, 2010, 93, 451-457.	1.2	23
82	Conformations of Phenylalanine in the Tripeptides AFA and GFG Probed by Combining MD Simulations with NMR, FTIR, Polarized Raman, and VCD Spectroscopy. Journal of Physical Chemistry B, 2010, 114, 3965-3978.	1.2	23
83	Cytochrome c: A Multifunctional Protein Combining Conformational Rigidity with Flexibility. New Journal of Science, 2014, 2014, 1-28.	1.0	23
84	Conformational Properties of Nickel(II)meso-Tetraphenylporphyrin in Solution. Raman Dispersion Spectroscopy Reveals the Symmetry of Distortions for a Nonplanar Conformer. Journal of Physical Chemistry A, 1997, 101, 5997-6007.	1.1	22
85	Dynamics of Various Metal-Octaethylporphyrins in Solution Studied by Resonance Raman and Low-Temperature Optical Absorption Spectroscopies. Role of the Central Metal. Journal of Physical Chemistry B, 1998, 102, 6612-6620.	1.2	22
86	Salt as a catalyst in the mitochondria: returning cytochrome c to its native state after it misfolds on the surface of cardiolipin containing membranes. Chemical Communications, 2014, 50, 3674-3676.	2.2	22
87	Do Molecular Dynamics Force Fields Capture Conformational Dynamics of Alanine in Water?. Journal of Chemical Theory and Computation, 2020, 16, 510-527.	2.3	22
88	Non-planar heme deformations and excited state displacements in horseradish peroxidase detected by Raman spectroscopy at Soret excitation. Journal of Raman Spectroscopy, 2005, 36, 363-375.	1.2	21
89	The conformations adopted by the octamer peptide (AAKA)2 in aqueous solution probed by FTIR and polarized Raman spectroscopy. Journal of Raman Spectroscopy, 2006, 37, 248-254.	1.2	21
90	Anomalous Conformational Instability and Hydrogel Formation of a Cationic Class of Self-Assembling Oligopeptides. Macromolecules, 2010, 43, 7800-7806.	2.2	21

#	Article	IF	CITATIONS
91	Probing conformational propensities of histidine in different protonation states of the unblocked glycylâ€histidylâ€glycine peptide by vibrational and NMR spectroscopy. Journal of Raman Spectroscopy, 2016, 47, 1063-1072.	1.2	21
92	Conformational Distortions of Metalloporphyrins with Electron-Withdrawing NO2Substituents at Different Meso Positions. A Structural Analysis by Polarized Resonance Raman Dispersion Spectroscopy and Molecular Mechanics Calculations. Journal of Physical Chemistry A, 2001, 105, 6680-6694.	1.1	19
93	Energy Landscapes Associated with the Self-Aggregation of an Alanine-Based Oligopeptide (AAKA) ₄ . Journal of Physical Chemistry B, 2009, 113, 6054-6061.	1.2	19
94	pH-Induced Switch between Different Modes of Cytochrome <i>c</i> Binding to Cardiolipin-Containing Liposomes. ACS Omega, 2019, 4, 1386-1400.	1.6	19
95	Triaspartate: A Model System for Conformationally Flexible DDD Motifs in Proteins. Journal of Physical Chemistry B, 2012, 116, 5160-5171.	1.2	18
96	A new interpretation of the structure and solvent dependence of the far UV circular dichroism spectrum of short oligopeptides. Chemical Communications, 2019, 55, 5701-5704.	2.2	18
97	Construction and comparison of the statistical coil states of unfolded and intrinsically disordered proteins from nearest-neighbor corrected conformational propensities of short peptides. Molecular BioSystems, 2016, 12, 3294-3306.	2.9	17
98	Water-Mediated Electronic Structure of Oligopeptides Probed by Their UV Circular Dichroism, Absorption Spectra, and Time-Dependent DFT Calculations. Journal of Physical Chemistry B, 2020, 124, 2579-2590.	1.2	17
99	Electronic and Vibronic Contributions to the Band Splitting in Optical Spectra of Heme Proteins. Journal of Physical Chemistry B, 2001, 105, 7064-7073.	1.2	16
100	Environment-Controlled Interchromophore Charge Transfer Transitions in Dipeptides Probed by UV Absorption and Electronic Circular Dichroism Spectroscopy. Journal of Physical Chemistry B, 2006, 110, 13235-13241.	1.2	16
101	Microperoxidase 11: a model system for porphyrin networks and heme–protein interactions. Journal of Biological Inorganic Chemistry, 2009, 14, 1289-1300.	1.1	16
102	Simulation of IR, Raman and VCD amide I band profiles of self-assembled peptides. Spectroscopy, 2010, 24, 25-36.	0.8	16
103	Method for the evaluation of normal modes and molecular mechanics with reduced sets of force constants. 1. Principles and reliability test. Journal of Raman Spectroscopy, 1999, 30, 3-28.	1.2	15
104	Asymmetric band profile of the Soret band of deoxymyoglobin is caused by electronic and vibronic perturbations of the heme group rather than by a doming deformation. Journal of Chemical Physics, 2007, 127, 135103.	1.2	15
105	pH Dependence of Ferricytochrome <i>c</i> Conformational Transitions during Binding to Cardiolipin Membranes: Evidence for Histidine as the Distal Ligand at Neutral pH. Journal of Physical Chemistry Letters, 2017, 8, 1993-1998.	2.1	15
106	Clycine in Water Favors the Polyproline II State. Biomolecules, 2020, 10, 1121.	1.8	15
107	Inâ€plane deformations of the heme group in native and nonnative oxidized cytochrome <i>c</i> probed by resonance Raman dispersion spectroscopy. Journal of Raman Spectroscopy, 2011, 42, 917-925.	1.2	14
108	Ionized Trilysine: A Model System for Understanding the Nonrandom Structure of Poly- <scp>l</scp> -lysine and Lysine-Containing Motifs in Proteins. Journal of Physical Chemistry B, 2012, 116, 8084-8094.	1.2	14

#	Article	IF	CITATIONS
109	The (Not Completely Irreversible) Population of a Misfolded State of Cytochrome c under Folding Conditions. Biochemistry, 2013, 52, 1397-1408.	1.2	14
110	Autoxidation of Reduced Horse Heart Cytochrome <i>c</i> Catalyzed by Cardiolipin-Containing Membranes. Journal of Physical Chemistry B, 2016, 120, 12219-12231.	1.2	14
111	Probing the Conformation-Dependent Preferential Binding of Ethanol to Cationic Glycylalanylglycine in Water/Ethanol by Vibrational and NMR Spectroscopy. Journal of Physical Chemistry B, 2017, 121, 5744-5758.	1.2	14
112	Short peptides as predictors for the structure ofÂpolyarginine sequences in disordered proteins. Biophysical Journal, 2021, 120, 662-676.	0.2	14
113	Regulation of mast cells? secretory response by co-clustering the Type 1 Fc? receptor with the mast cell function-associated antigen. European Journal of Immunology, 2005, 35, 1621-1633.	1.6	13
114	Outâ€ofâ€plane deformations of the heme group in different ferrocytochrome c proteins probed by resonance Raman spectroscopy. Journal of Raman Spectroscopy, 2008, 39, 1848-1858.	1.2	13
115	Entropy reduction in unfolded peptides (and proteins) due to conformational preferences of amino acid residues. Physical Chemistry Chemical Physics, 2014, 16, 22527-22536.	1.3	13
116	Anticooperative Nearest-Neighbor Interactions between Residues in Unfolded Peptides andÂProteins. Biophysical Journal, 2018, 114, 1046-1057.	0.2	13
117	Exploring the gel phase of cationic glycylalanylglycine in ethanol/water. I. Rheology and microscopy studies. Journal of Colloid and Interface Science, 2020, 564, 499-509.	5.0	13
118	The Fe2+-HisF8 Raman Band Shape of Deoxymyoglobin Reveals Taxonomic Conformational Substates of the Proximal Linkage. Biophysical Journal, 2001, 81, 1624-1631.	0.2	12
119	Conformational analysis of tetrapeptides by exploiting the excitonic coupling between amide I modes. Journal of Raman Spectroscopy, 2004, 35, 586-591.	1.2	12
120	Conformational Stability of Cytochrome c Probed by Optical Spectroscopy. Methods in Enzymology, 2009, 466, 109-153.	0.4	12
121	Near-exact enthalpy–entropy compensation governs the thermal unfolding of protonation states of oxidized cytochrome c. Journal of Biological Inorganic Chemistry, 2014, 19, 1181-1194.	1.1	12
122	Ultra-Long Crystalline Red Phosphorus Nanowires from Amorphous Red Phosphorus Thin Films. Angewandte Chemie, 2016, 128, 12008-12012.	1.6	12
123	Formation of peptide-based oligomers in dimethylsulfoxide: identifying the precursor of fibril formation. Soft Matter, 2020, 16, 7860-7868.	1.2	12
124	Short Peptides as Tunable, Switchable, and Strong Gelators. Journal of Physical Chemistry B, 2021, 125, 6760-6775.	1.2	12
125	Investigation of haem-protein coupling and structural heterogenity in myoglobin and haemoglobin by resonance Raman spectroscopy. Journal of Raman Spectroscopy, 1992, 23, 539-550.	1.2	11
126	Reply to Comment on "Vibrational Assignments oftrans-N-Methylacetamide and Some of Its Deuterated Isotopomers from Band Decomposition of IR, Visible, and Resonance Raman Spectra― Journal of Physical Chemistry A, 1997, 101, 3992-3994.	1.1	11

#	Article	IF	CITATIONS
127	Functionally Relevant Electric-Field Induced Perturbations of the Prosthetic Group of Yeast FerrocytochromecMutants Obtained from a Vibronic Analysis of Low-Temperature Absorption Spectra. Journal of Physical Chemistry B, 2006, 110, 12155-12161.	1.2	11
128	Structural Destabilization of Azurin by Imidazolium Chloride Ionic Liquids in Aqueous Solution. Journal of Physical Chemistry B, 2019, 123, 6933-6945.	1.2	11
129	Raman dispersion spectroscopy probes heme distortions in deoxyHb-trout IV involved in its T-state Bohr effect. Biophysical Journal, 1993, 64, 1194-1209.	0.2	10
130	Parameters determining the stimulatory capacity of the type I Fcε-receptor. Immunology Letters, 1999, 68, 59-69.	1.1	10
131	Static Normal Coordinate Deformations of the Heme Group in Mutants of Ferrocytochrome c from Saccharomyces cerevisiae Probed by Resonance Raman Spectroscopy. Journal of Physical Chemistry B, 2007, 111, 6527-6533.	1.2	10
132	Exploring the thermal reversibility and tunability of a low molecular weight gelator using vibrational and electronic spectroscopy and rheology. Soft Matter, 2019, 15, 3418-3431.	1.2	10
133	Mast cell stimulation by co-clustering the type I Fcε-receptors with mast cell function-associated antigens. Immunology Letters, 1999, 68, 71-78.	1.1	9
134	Heme Structural Perturbation of PEG-Modified Horseradish Peroxidase C in Aromatic Organic Solvents Probed by Optical Absorption and Resonance Raman Dispersion Spectroscopy. Biophysical Journal, 2003, 84, 3285-3298.	0.2	9
135	Cu(II) and Ni(II) Interactions with the Terminally Blocked Hexapeptide Ac-Leu-Ala-His-Tyr-Asn-Lys-amide Model of Histone H2B (80–85). Bioinorganic Chemistry and Applications, 2008, 2008, 1-10.	1.8	9
136	Using spectroscopic tools to probe porphyrin deformation and porphyrin-protein interactions. Journal of Porphyrins and Phthalocyanines, 2011, 15, 312-337.	0.4	9
137	Different Degrees of Disorder in Long Disordered Peptides Can Be Discriminated by Vibrational Spectroscopy. Journal of Physical Chemistry B, 2013, 117, 6927-6936.	1.2	9
138	Investigating the Formation of a Repulsive Hydrogel of a Cationic 16mer Peptide at Low Ionic Strength in Water by Vibrational Spectroscopy and Rheology. Journal of Physical Chemistry B, 2016, 120, 10079-10090.	1.2	9
139	Ferrocyanideâ€Mediated Photoreduction of Ferricytochromeâ€C Utilized to Selectively Probe Nonâ€native Conformations Induced by Binding to Cardiolipinâ€Containing Liposomes. Chemistry - A European Journal, 2017, 23, 1151-1156.	1.7	9
140	Exploring the gel phase of cationic glycylalanylglycine in ethanol/water. II. Spectroscopic, kinetic and thermodynamic studies. Journal of Colloid and Interface Science, 2020, 573, 123-134.	5.0	9
141	Do molecular dynamics force fields accurately model Ramachandran distributions of amino acid residues in water?. Physical Chemistry Chemical Physics, 2022, 24, 3259-3279.	1.3	9
142	The combined use of amide I bands in polarized Raman, IR, and vibrational dichroism spectra for the structure analysis of peptide fibrils and disordered peptides and proteins. Journal of Raman Spectroscopy, 2021, 52, 2479-2499.	1.2	8
143	Repeating Aspartic Acid Residues Prefer Turn-like Conformations in the Unfolded State: Implications for Early Protein Folding. Journal of Physical Chemistry B, 2021, 125, 11392-11407.	1.2	8
144	Vibrational Analysis of Metalloporphyrins with Electron-Withdrawing NO2Substituents at Different Meso Positions. Journal of Physical Chemistry A, 2001, 105, 6668-6679.	1.1	7

#	Article	IF	CITATIONS
145	Interaction of a Tripeptide with Cesium Perfluorooctanoate Micelles. Journal of Physical Chemistry B, 2008, 112, 1251-1261.	1.2	7
146	Probing the replacement of water by dimethyl sulfoxide in the hydration shell of N-methylacetamide by FTIR-spectroscopy. Vibrational Spectroscopy, 2017, 92, 251-258.	1.2	7
147	The tripeptide GHG as an unexpected hydrogelator triggered by imidazole deprotonation. Soft Matter, 2020, 16, 4110-4114.	1.2	7
148	Structural Analysis of Unfolded Peptides by Raman Spectroscopy. Methods in Molecular Biology, 2012, 895, 315-346.	0.4	6
149	Vibrational analysis of Ni(II)- and Cu(II)-octamethylchlorin by polarized resonance Raman and Fourier transform infrared spectroscopy. Journal of Raman Spectroscopy, 2001, 32, 521-541.	1.2	5
150	Orientation of Oligopeptides in Self-Assembled Monolayers Inferred from Infrared Reflection–Absorption Spectroscopy. Journal of Physical Chemistry B, 2019, 123, 860-868.	1.2	5
151	Intrinsic Conformational Dynamics of Alanine in Water/Ethanol Mixtures: An Experiment-Driven Molecular Dynamics Study. Journal of Physical Chemistry B, 2020, 124, 11600-11616.	1.2	5
152	Structure Analysis of Unfolded Peptides I: Vibrational Circular Dichroism Spectroscopy. Methods in Molecular Biology, 2012, 895, 271-313.	0.4	3
153	Photoreduction of ferricytochrome c in the presence of potassium ferrocyanide. Photochemical and Photobiological Sciences, 2018, 17, 1462-1468.	1.6	3
154	Concentration Dependence of a Hydrogel Phase Formed by the Deprotonation of the Imidazole Side Chain of Glycylhistidylglycine. Langmuir, 2021, 37, 6935-6946.	1.6	3
155	Randomizing of Oligopeptide Conformations by Nearest Neighbor Interactions between Amino Acid Residues. Biomolecules, 2022, 12, 684.	1.8	3
156	Exploring Nearest Neighbor Interactions and Their Influence on the Gibbs Energy Landscape of Unfolded Proteins and Peptides. International Journal of Molecular Sciences, 2022, 23, 5643.	1.8	3
157	The impact of thermal history on the structure of glycylalanylglycine ethanol/water gels. Journal of Peptide Science, 2021, 27, e3305.	0.8	2
158	Polarized Resonance Raman Spectroscopy Reveals Two Different Conformers of Metallo(II)octamethylchlorins in CS2. Journal of Physical Chemistry B, 1999, 103, 9777-9781.	1.2	1